Title
The Majoron model and stellar collapse

Journal
The Astrophysical Journal, 332(2)

ISSN
0004-637X

Authors
Fuller, GM
Mayle, R
Wilson, JR

Publication Date
1988-09-01

DOI
10.1086/166695

Peer reviewed

THE ASTROPHYSICAL JOURNAL, 332:826–841, 1988 September 15

THE MAJORON MODEL AND STELLAR COLLAPSE

G. M. FULLER, R. MAYLE, AND J. R. WILSON
Institute of Geophysics and Planetary Physics, University of California, Lawrence Livermore National Laboratory
Received 1988 February 24; accepted 1988 March 15

ABSTRACT

We study stellar core collapse with the Gelmini-Roncadelli-Georgi-Glashow-Nussinov Majoron model of the weak interaction. The large-scale lepton number nonconservation in neutrino-neutrino interactions, which is inherent in this model, leads to entropy production in the infall epoch of the presupernova star and a thermal bounce of the core at subnuclear density. This result is quite different from the standard low-entropy model of stellar collapse and occurs for values of the dimensionless coupling constant, g, characterizing the Majoron model, $g \geq 3 \times 10^{-5}$. We consider three different scenarios for the thermalization of neutrinos and majorons. In the case where total neutrino plus majoron number is not conserved we find that the spectrum of neutrinos resulting after core bounce may be inconsistent with the observed neutrino spectrum from SN 1987A whenever $g \geq 3 \times 10^{-4}$.

Subject headings: elementary particles — neutrinos — stars: collapsed — stars: supernovae

I. INTRODUCTION

Many attempts to extend the Weinberg-Salam-Glashow theory of the weak interaction to include small Majorana mass terms for neutrinos result in theories in which there are lepton number violating reactions (Gelmini and Roncadelli 1981; Georgi, Glashow, and Nussinov 1982). It has been pointed out by several authors that such lepton number violating reactions can have a major impact on the standard model of the collapse of the cores of massive stars (10–50 $M_\odot$): notably, the weak interaction model of Gelmini and Roncadelli (1981) was suggested to result in large-scale lepton number violation and entropy generation in a collapsing stellar core with trapped neutrinos (Kolb, Tubbs, and Dicus 1982; Dicus, Kolb, and Tubbs 1983).

Recently there have been several attempts to use neutrinoless double beta-decay experiments to investigate the existence of the massless Goldstone boson, the majoron, associated with these lepton number-violating theories of the weak interaction. Notably, Avignone *et al.* (1987) have found some evidence for the existence of the majoron in such an experiment, and these authors find a preliminary value of the dimensionless coupling constant (to be defined in the next section) $g \approx 8 \times 10^{-4}$. Other double beta-decay experiments would give smaller upper limits (Elliot, Hahn, and Moe 1987; Caldwell 1988; Alston-Garnjost *et al.* 1988). Lepton number violation at the level suggested by the Avignone *et al.* (1987) value of g would completely change the current picture of stellar core collapse, as we will show below.

The standard model of the collapse of the Fe core of a presupernova star relies on the low entropy of the material in the collapse (Bethe *et al.* 1979). Kolb, Tubbs, and Dicus (1982) suggested that the lepton number violating reactions associated with a weak interaction theory like that of Gelmini and Roncadelli (1981) can lead to entropy generation by unblocking electron capture phase space and "rearranging" lepton number from residing only in e^- and ν_e to $(\nu_\mu)_L$, $(\nu_\mu)_R$, $(\nu_\tau)_L$, and $(\nu_\tau)_R$. The estimates of electron capture rates and neutrino transformation rates in that work were at best based on simple one-zone collapse models like that of Fuller (1982) and not on self-consistent models with a detailed equation of state and neutrino transport. Thus, Kolb, Tubbs, and Discus (1982) posed a problem for astrophysicists: given the Gelmini-Roncadelli model of the weak interaction, does the collapse of the iron core of a star lead to a supernova explosion?

In what follows we will attempt to answer this question and suggest that the spectrum of neutrinos produced after the explosion may not be consistent with the neutrino observations of SN 1987A (Bionta *et al.* 1987, IMB; Hirata *et al.* 1987, Kamiokande). This latter result depends on the way in which the neutrinos and majorons thermalize outside the collapsing core. These issues, as well as the details of entropy generation, will be discussed below.

II. THE MAJORON MODEL AND NEUTRINO INTERACTIONS

There are currently many models of the weak interaction which extend the standard Weinberg-Salam-Glashow theory to include majorana mass terms for the neutrinos by postulating a symmetry associated with either lepton number (Gelmini and Roncadelli 1981; Georgi, Glashow, and Nussinov 1982) or lepton families (see Grinstein, Preskill, and Wise 1985) which is spontaneously broken at low temperature. We shall refer to all such theories as "majoron models" even though the term majoron is strictly associated with only the former class of theories. Hereafter, we shall focus on the Gelmini-Roncadelli-Georgi-Glashow-Nussinov (GRN) majoron model.

The GRN majoron model associates lepton number with a global $U(1)$ symmetry. At temperatures higher than the critical temperature for symmetry restoration lepton number is absolutely conserved: electron, muon, and tau lepton numbers are separately conserved, and the standard weak interactions obtain.

At low temperatures this symmetry is spontaneously broken, leading to a triplett of Higg's fields Λ, and a massless Goldstone

boson, or majoron particle ϕ. The Higg's field Λ is a triplett of boson fields,

$$\Lambda = \begin{pmatrix} \Lambda^{--} \\ (\Lambda^{-}) \\ \Lambda^{\circ} \end{pmatrix} , \tag{1}$$

which has a Yukawa coupling to lepton fields $l_L \equiv (\nu_L, e_L)$,

$$L = -g\overline{(l_L)}\boldsymbol{\tau} \cdot \bar{\Lambda}(l_L) , \tag{2}$$

where g is an arbitrary constant and $\boldsymbol{\tau}$ are the Pauli spin matrices. When the lepton number $U(1)$ symmetry is broken, Λ° acquires a vacuum expectation value $\langle \Lambda^{\circ} \rangle$. The spin-zero degrees of freedom in this case are the massless majoron ϕ and a neutral "majoron" ρ with mass $m_\rho \approx \langle \Lambda^{\circ} \rangle$ ($m_\rho \leq 100$ keV from the existence of red giant stars; Georgi, Glashow, and Nussinov 1982).

The masses of neutrinos of flavor i are then

$$m_{\nu_i} \approx g_i \langle \Lambda^{\circ} \rangle , \tag{3}$$

where g_i is related to the g in equation (2). Gelmini and Roncadelli (1981) suggested that the g_i should lie in the range

$$10^{-6} \leq g_i \leq 10^{-2} \tag{4}$$

in order that neutrinos have masses in an "interesting" range: 10^{-7} eV $\leq m_\nu \leq 1$ keV.

In what follows we will assume that each neutrino flavor has the same g. Although this is a completely arbitrary choice, it suffices to illustrate the changes in the standard model of stellar collapse due to lepton number nonconservation.

The Lagrangian in equation (2) implies that the lepton processes involving the usual charged current and neutral current are the same as those of the standard weak interactions up to corrections of order (m_ν/m_l), where m_l is the mass of a charged lepton. Also, if a lepton number $L = +1\,(-1)$ is assigned to left-handed (right-handed) neutrinos, $\nu_L(\nu_R)$, then this lepton number is conserved by the usual charged current and neutral current ($W^{\pm}$, Z exchange) to order (m_ν/E_ν), where E_ν is the neutrino total energy. Given the range of neutrino masses implied by equation (4) and the fact that typical neutrino energies of interest in stellar collapse are of order $E_\nu \approx 10$ MeV, we can conclude that lepton number is conserved to high accuracy by $W^{\pm}$ and Z° exchange.

Lepton number is not conserved in the spontaneously broken sector of the GRN theory when neutrinos interact with the ρ and ϕ majorons. The interaction Lagrangian in this case is

$$L_{\text{int}} = -ig\overline{(\nu_L)}\gamma_5 \nu_L \phi + g\overline{(\nu_L)}\nu_L \rho , \tag{5}$$

where the $\overline{(\nu_L)}$ denotes the adjoint and charge conjugate of ν_L. Note that no lepton number can be associated with the majorons in equation (5). Processes like neutrino scattering via majoron exchange shown in Figure 1*a* can flip neutrino helicities so that lepton number is violated by two units, likewise for other two-to-two processes like majoron scattering into neutrinos (Fig. 1*b*) and neutrino scattering into majorons (Fig. 1*c*).

The cross section for majoron mediated neutrino-neutrino or majoron-majoron scattering is then

$$\sigma_\phi \approx \alpha_\phi^2 E_\nu^{-2} , \tag{6a}$$

where $\alpha_\phi = g^2/4\pi$ and E_ν is a typical neutrino or majoron energy. Since a standard weak interaction process involving neutrino

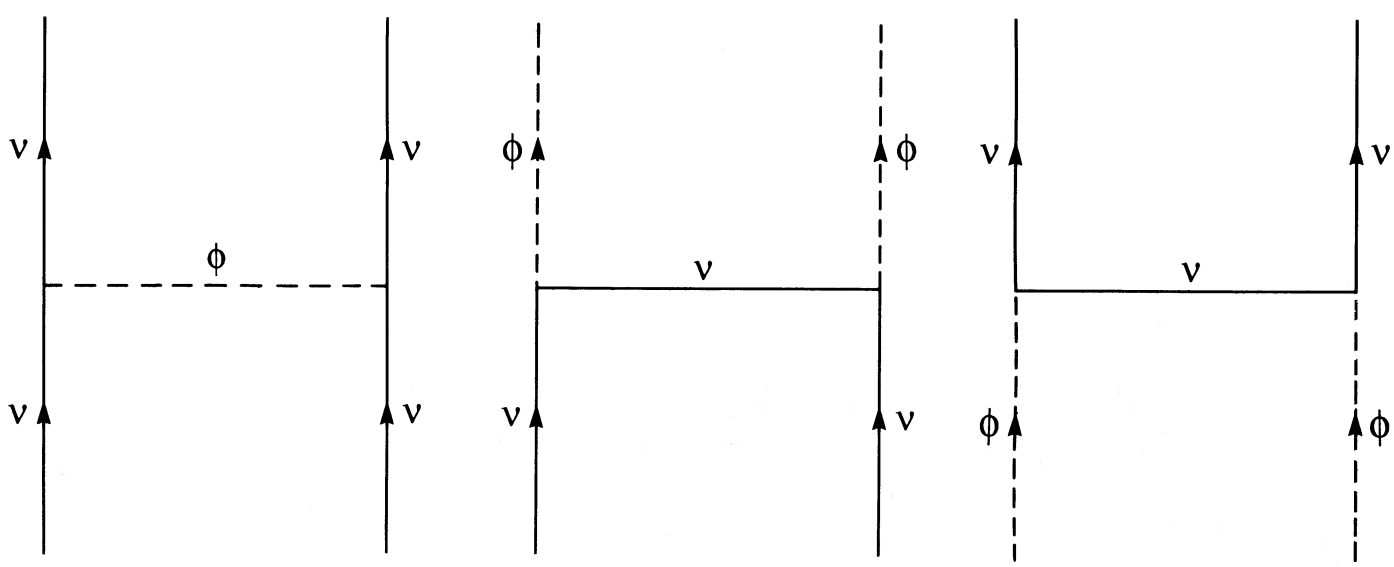

FIG. 1*a* FIG. 1*b* FIG. 1*c*

FIG. 1.—Two-to-two processes involving majorons, ϕ, and neutrinos, ν: (*a*) neutrino-neutrino scattering mediated by majoron exchange; (*b*) neutrino annihilation into majorons; (*c*) majoron annihilation into neutrinos.

scattering has a cross section that is roughly $\sigma_w \approx G_F^2 E_\nu^2$ (where G_F is the Fermi constant) the relative ratio of cross sections for neutrino scattering via majoron exchange to standard neutrino cross sections is (Kolb, Tubbs, and Dicus 1982)

$$\frac{\sigma_\phi}{\sigma_w} \approx \frac{g^4}{(G_F^2 E_\nu^4)} . \tag{6b}$$

For typical neutrino energies during the infall epoch of stellar collapse ($E_\nu \approx 10$ MeV) we see that the neutrino-majoron interactions dominate the standard weak interactions whenever $g \geq 3 \times 10^{-5}$.

In what follows we will assume that $g \geq 3 \times 10^{-5}$ so that the Kolb, Tubbs, and Dicus (1982) picture of the initial mode obtains. In this picture the Fe core of the presupernova star collapses at low entropy as in the standard model until the central density reaches $\rho \geq 4 \times 10^{11}$ g cm^{-3} where the neutrinos begin to be trapped. As the neutrinos are trapped, and the neutrino number density rises, the majoron interactions become increasingly important. The neutrino and majoron distribution functions are driven to thermal equilibrium on a time scale short compared to the weak equilibrium time scale ($\tau_{\rm weak} \geq 10^{-5}$ s). The neutrinos communicate with each other through the relatively strong majoron interaction. On the other hand, the neutrinos "feel" the matter only through the standard weak interaction, so that although the neutrino distribution functions are rapidly driven to *thermal* equilibrium by majoron interactions, *chemical* equilibrium with electrons is achieved only on a relatively long weak-interaction time scale. Entropy is generated as the system of neutrinos, majorons, electrons, positrons, neutrons, protons, and nuclei relaxes to equilibrium. We will discuss the details of entropy generation and changes in lepton number in § IV.

We further note, however, that the manner in which the neutrinos and majorons equilibrate among themselves will determine the final distribution of neutrino energies after core bounce. In particular, we will show in § IV that the neutrino energies are sensitive to whether or not *total* neutrino plus majoron number is conserved. Note that the two-to-two processes shown in Figures 1*a*–1*c* all conserve total neutrino plus majoron number. These processes also have the large rates associated with the majoron exchange cross section in equation (6a). By contrast, the three-body processes shown in Figures 2*a* and 2*c* clearly change total neutrino plus majoron number. The rates of these processes are slow at lower densities because of phase space limitations. Total neutrino plus majoron number is not conserved in annihilation/bremsstrahlung reactions like that shown in Figure 2*b* (Fig. 2*b* shows neutrino annihilation into majorons; other topologies of this basic vertex give majoron emission in neutrino bremsstrahlung). The rates of these processes are smaller than for the two-to-two processes because the majoron mass is small compared to typical neutrino energies. A typical "decay" rate (or bremsstrahlung rate) of neutrino into a neutrino plus majoron is (Frieman 1987)

$$\lambda = \frac{g^2 m_\phi^2}{16\pi E_\nu} , \tag{7a}$$

where m_ϕ is a typical majoron or neutrino mass and E_ν is again a typical neutrino or majoron energy. We note that although the vacuum mass of some of the scalar degrees of freedom associated with the majoron are zero, others (corresponding to the ρ mentioned above) are nonzero and could be as large as 100 keV as stated previously. Furthermore, in the dense plasma of neutrinos, majorons, electrons, and nucleons which obtains in the collapsing stellar core neutrinos and majorons can have appreciable effective masses due to forward scattering processes. Fuller *et al.* (1987) showed that these processes each contribute ~ 1 keV in effective mass

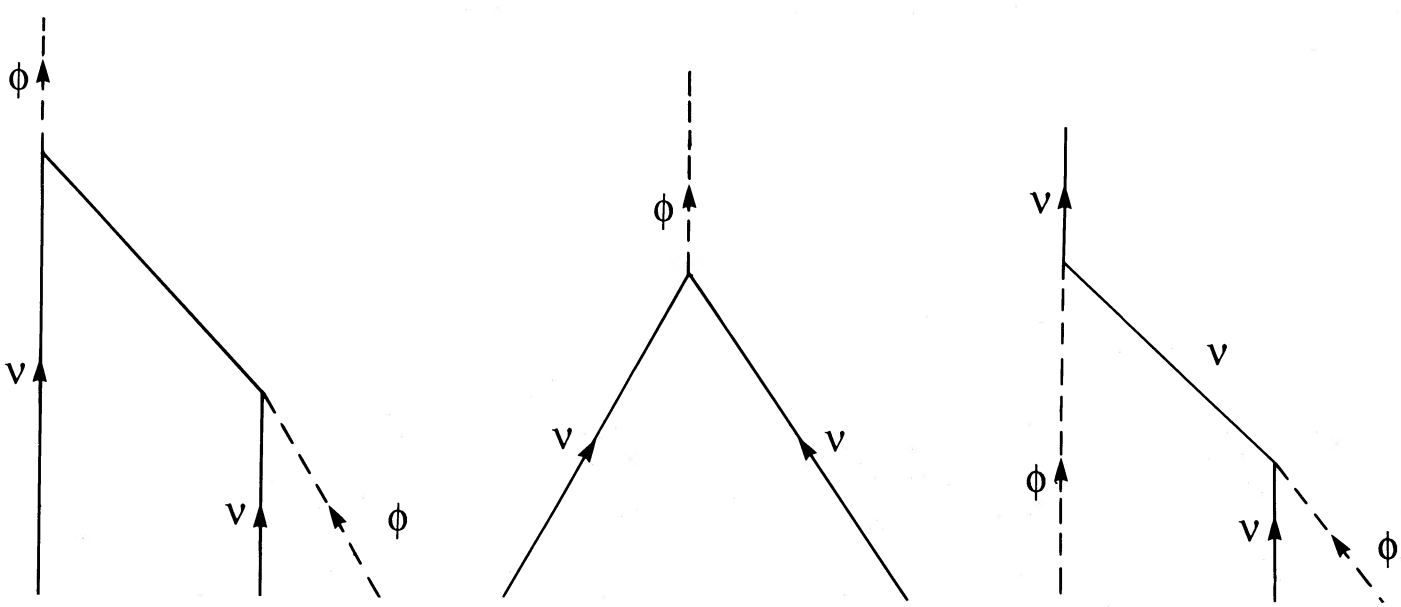

FIG. 2*a* FIG. 2*b* FIG. 2*c*

FIG. 2.—Number changing processes involving neutrinos and majorons: (*a*) three-body annihilation into majorons; (*b*) neutrino annihilation into a majoron (other time ordering and topologies give neutrino decay into neutrino plus majoron, etc.); (*c*) three-body annihilation of neutrinos and majorons into a neutrino.

to neutrinos. Typical mass differences between neutrinos or majorons should then be of order 1–10 keV due to the standard weak interaction processes, with further contributions from majoron exchange effects.

From equation (7a) the time scale for majoron plus neutrino number changing reactions is then

$$\tau_{\phi\nu} \approx (3.3 \times 10^{-20}\ \mathrm{s})\left(\frac{E_\nu}{\mathrm{MeV}}\right)\left[g\left(\frac{m_\phi}{\mathrm{MeV}}\right)\right]^{-2}, \tag{7b}$$

which gives $\tau \approx 3 \times 10^{-5}$ s for $m_\phi \approx 1$ keV, $g \approx 10^{-4}$, and $E_\nu = 10$ MeV.

In order for neutrino plus majoron number to change rapidly enough to effect the core collapse physics the total number changing time scale must be short compared to a weak-equilibrium time scale, τ_{weak}. At the photosphere $\tau_{\mathrm{weak}} \approx 3 \times 10^{-5}$ s. Given the range of possible neutrino energies and majoron effective masses then, we conclude that neutrino plus majoron number nonconservation is important always when $g \geq 10^{-4}$. In subsequent sections we will discuss majoron and neutrino thermalization, both in the limit where majoron plus neutrino number is conserved and where it is not.

III. DESCRIPTION OF THE NUMERICAL METHOD

For a general discussion of the numerical code used to model supernovae see Bowers and Wilson (1982) (in this section abbreviated as BW) and Mayle (1985). A paper is currently in preparation that describes the supernova code in its present form, but the other two references contain much of the detail and spirit of the approximations made to the physics now modeled in the code. We will need to describe in detail here, however, the way in which the neutrino transport is modified by additional reactions that neutrinos have with majorons. One assumption is that the six neutrinos, ν_e, $\bar{\nu}_e$, ν_μ, $\bar{\nu}_\mu$, ν_τ, $\bar{\nu}_\tau$ become thoroughly mixed in flavor space by the interactions with majorons on time scales very short compared to dynamical time scales or weak interaction time scales. Thus, we need to follow only one neutrino species, as the other five are assumed represented by similar neutrino distribution functions (to be defined below). Since the different flavor neutrinos and their antiparticles interact (via the weak interaction) with matter in dissimilar ways, we have defined average cross sections and an average mean free path (described in detail below) for use in our single transport equation.

We also assume that the neutrinos become thermalized among themselves and with the majoron particles very quickly compared with the thermalization time scales implied by the weak interaction. The equation we solve is

$$\frac{\partial F}{\partial t} = \nabla \cdot (D\nabla F) + \left.\frac{\partial F}{\partial t}\right|_\phi + \left.\frac{\partial F}{\partial t}\right|_\beta + \left.\frac{\partial F}{\partial t}\right|_{\mathrm{hydro}}, \tag{8}$$

where F is a generic neutrino distribution function to be defined below, and where the first term on the right-hand side of equation (8) represents the diffusion of the neutrinos, the second takes into account changes in F due to interactions with majorons, the third term includes changes in F due to scattering and emission and absorption reactions with the matter via the weak interaction, and the fourth term takes into account changes in F due to material compression of the neutrino field. If f is the Fermi-Dirac distribution function for the neutrinos such that in thermal equilibrium with themselves

$$f = \left[\exp\left(\frac{\epsilon - \mu_\nu}{T_\nu}\right) + 1\right]^{-1}, \tag{9}$$

where μ_ν is the neutrino chemical potential, T_ν is the neutrino temperature, and ϵ is the neutrino energy, then our distribution function F is defined to be

$$F = w\alpha f \epsilon^3, \tag{10}$$

where $w = 6$ is a weight that represents all six neutrino fields combined into one super neutrino distribution function, and $\alpha = 1/[2\pi^2(\hbar c)^3]$. The units of F are inverse volume, so $\int F\, d\epsilon$ is the total energy density in all types of neutrinos and $\int F(d\epsilon/\epsilon)$ is the total neutrino number density.

The diffusion coefficient D is a function of the transport mean free path of the neutrinos, λ, which we take to be an average of the individual ν_e, $\bar{\nu}_e$, ν_μ, $\bar{\nu}_\mu$, ν_τ, $\bar{\nu}_\tau$ mean free paths. We take $\lambda = (\lambda_{\nu_e} + \lambda_{\bar{\nu}_e} + 4\lambda_{\mu\tau})/6$ (see BW for details on the construction of the mean free path for the various neutrino flavors and their antiparticles). We have written equation (8) in an approximation that neglects the effects of general relativity for ease in discussion only, the full effects of general relativity are included in the transport equation used in the supernova code.

We now turn to a discussion of the remaining terms on the right-hand side of equation (8). As previously mentioned, the second term $\partial F/\partial t\,|_\phi$ represents changes in F due to interaction with majorons. This term depends on the way in which we approximate the Gelmini-Roncadelli-Nussinov majoron model in our calculations. We have made three different approximations, depending on the size of the coupling constant in the Gelmini-Roncadelli-Nussinov model. Model 1 assumes reactions such as $\nu + \nu \rightarrow \phi$ and $\nu + \nu \rightarrow \phi + \phi$ (see Figs. 1 and 2) are virtually instantaneous, and imply $\mu_\nu = \mu_\phi = 0$, where ϕ denotes a majoron, ν a neutrino, μ_ν is the neutrino chemical potential, and μ_ϕ is the majoron chemical potential. Note that neutrino and majoron chemical potentials are always defined in this model since we assume the neutrinos and majorons are in thermal equilibrium at temperature T_ν and chemical potential μ_ν. However, the neutrinos and majorons are not assumed to be in thermal equilibrium with the matter. For model 1, the term $\partial F/\partial t\,|_\phi$ is the change needed in F to bring it into a thermal distribution at temperature T_ν. We assume ϕ is a spin zero boson with energy density given by $E = \frac{1}{2}aT_\nu^4$ (a is 1.37×10^{26} if T_ν is in MeV), and solve for T_ν by requiring the energy density of the neutrinos and majorons to be given by

$$\text{Energy Density} = \int F\, d\epsilon + \tfrac{1}{2}aT_\nu^4, \tag{11}$$

where $F = 6\alpha\epsilon^3/[\exp(\epsilon/T_\nu) + 1]$. The majoron will exert a pressure $(\frac{1}{6}aT_\nu^4)$, and this contribution to the total pressure is included in the hydrodynamics.

Model 2 assumes that reactions of the type $\nu + \nu \to \phi + \phi$ are the only majoron production reactions to occur. In this case, even though the usual lepton number is not conserved, total particle number (number of neutrinos + majorons) is conserved. Therefore, a negative nonzero value of μ_ν is possible. We also must allow for a Bose condensate of majorons to exist if $\mu_\phi = \mu_\nu$ becomes equal to zero. The equations we solve for model 2 are

$$\frac{\partial}{\partial t}\left(\int F\, d\epsilon + \epsilon_\phi\right) = 0\,, \tag{12a}$$

$$\frac{\partial}{\partial t}\left(\int F\,\frac{d\epsilon}{\epsilon} + N_\phi + N_0\right) = 0\,, \tag{12b}$$

where

$$\epsilon_\phi = \alpha\int_{\mu_\nu}^{\infty}\frac{\epsilon^3 d\epsilon}{\exp\,[(\epsilon-\mu_\nu)/T_\nu]-1} = \frac{1}{2}\,aT_\nu^4\exp\left(\frac{\mu_\nu}{T_\nu}\right)h_e\left(\frac{\mu_\nu}{T_\nu}\right), \tag{13a}$$

$$N_\phi = \alpha\int_{\mu_\nu}^{\infty}\frac{\epsilon^2 d\epsilon}{\exp\,[(\epsilon-\mu_\nu)/T_\nu]-1} = \frac{1}{2}\,bT_\nu^3\exp\left(\frac{\mu_\nu}{T_\nu}\right)h_n\left(\frac{\mu_\nu}{T_\nu}\right), \tag{13b}$$

and $a = 1.37 \times 10^{26}$ and $b = 3.17 \times 10^{22}$ if T_ν is measured in MeV. The functions h_e and h_n are numerical fits to an exact integration of the Bose-Einstein distribution function representing the majoron (neglecting m_ϕ). We find

$$h_e = 0.924 + 0.076\exp(\mu_\nu/T_\nu)\,, \tag{14a}$$

$$h_n = 0.823 + 0.168\exp(3\mu_\nu/2T_\nu)\,, \tag{14b}$$

are good to a few percent. The quantity N_0 represents the number density of majorons present in the Bose condensate. We solve the system (12) for N_0, μ_ν, T_ν by first assuming $N_0 = 0$ and finding μ_ν and T_ν. If $\mu_\nu \le 0$, then we have a consistent solution and are finished. If $\mu_\nu > 0$, we resolve equation (12) by setting $\mu_\nu = 0$ and find T_ν from equation (12a); then N_0 follows from equation (12b).

Model 3 assumes that no free majorons are produced, but only act as virtual particles that mediate the thermalization of the neutrinos in neutrino scattering reactions. In this case the $\partial F/\partial t|_\phi$ term is taken into account by requiring that F be a neutrino distribution function in the form of equation (10) with neutrino temperature and chemical potential found such that both neutrino energy density and neutrino number density are preserved.

The third term in the right-hand side of equation (8), $\partial F/\partial t|_\beta$, takes into account changes in F due to weak interactions of neutrinos with baryons, electrons, and positrons. This term is discussed in BW: in this paper we will discuss changes in the term $\partial F/\partial t|_\beta$ induced by approximating six neutino fields with one superfield. Changes in F due to electron capture on heavy nuclei is done as in BW except that the term $f_e - F/\alpha\epsilon^3$ in equation (4.12) of that paper is replaced by $f_e - F/6\alpha\epsilon^3$ to take into account that only one-sixth of F, representing ν_e, participate in the reverse reaction. The quantity F also changes due to scattering with electron and positrons. An approximate treatment is used involving a Fokker-Planck equation as described in BW, equation (7). For the changes in F due to scattering with electrons and positrons (in the calculations done for this paper) we have used an average value for the relaxation times, τ_c, given by

$$\frac{1}{\tau_c} = \frac{1}{6}\left(\frac{1}{\tau_{\nu_e}} + \frac{1}{\tau_{\bar{\nu}_e}}\right) + \frac{2}{3}\,\frac{1}{\tau_{\nu_\mu}}\,, \tag{15}$$

where τ_{ν_e}, $\tau_{\bar{\nu}_e}$, τ_{ν_μ} are relaxation times for ν_e, $\bar{\nu}_e$, ν_μ scattering (see BW for the method of construction of these quantities).

For plasmon and pair production of neutrinos and the inverse reactions we use the method described in §VIII*e* of BW. We had previously included plasmon and pair production of election neutrinos and electron antineutrinos in the supernova code (see Mayle 1985), in the same spirit as the approximation found in BW, which only took pair and plasmon production of mu and tau neutrinos and their antiparticles into account. Note that the inverse reaction to pair and plasma production is inhibited outside the neutrinosphere since the neutrinos become free streaming and are not isotropically distributed in space. We use a multiplicative cutoff of the inverse reaction (i.e., neutrino-antineutrino annihilation into an electron-positron pair or plasmon) of the form $[1 + (\lambda/3)|(\partial \ln F/\partial r)|]^{-2}$ that reduces to unity in the diffuse limit and zero in the limit of free streaming. In formula (8.64a) for the $\dot{E}_{\rm th}$ and formula (8.65a) for $\dot{E}_{\rm Plas}$ found in BW we replace $(C_v - 1)^2$ with $C_v^2 + \frac{2}{3}(C_v - 1)^2$ for the calculations done in this paper. The $(C_v - 1)^2$ is correct for mu/tau neutrino and antineutrino production by pairs or the plasma process, and C_v^2 is correct for electron neutrino and electron antineutrino production by the pair or plasma process. The particular average we use represents the fact that two-thirds of our super distribution function, F, represents mu/tau neutrinos and antineutrinos, while one-half represents electron neutrinos and antineutrinos.

One final part of $\partial F/\partial t|_\beta$ is due to emission and absorption of electron neutrinos and antineutrinos on free baryons. We call this $\partial F/\partial t|_{\rm ea}$ and write it as follows:

$$\frac{\Delta\epsilon}{\epsilon}\,\frac{\partial F}{\partial t}\bigg|_{\rm ea} = c\sigma_{\rm ep}(2\alpha e^2 f_e\,\Delta e)n_p(1-f) + c\sigma_{ne} + (2\alpha\tilde{e}^2 f_e + \Delta\tilde{e})n_n(1-f) - c\sigma_{n\nu_e}(\alpha\epsilon^2\Delta\epsilon f)n_n(1-f_e) - c\sigma_{p\bar{\nu}_e}(\alpha\epsilon^2\Delta\epsilon f)n_p(1-f_{e^+})\,, \tag{16}$$

where the first term on the right-hand side comes from electron capture on protons, the second from positron capture on neutrons,

the third from electron neutrino capture on neutrons, and the fourth from electron antineutrino capture on protons. Note that f_e and f_{e^+} are Fermi-Dirac distribution functions for electrons and positrons, respectively, e is the electron energy, $\tilde{e}$ is the positron energy, f is defined from F by equation (10), and n_p and n_n are the number densities for free protons and free neutrons. The cross sections for neutrino interactions with free baryons are taken from Tubbs and Schram (1975) and are given by

$$\sigma_{\rm ep} = \frac{1.33}{2}\sigma_0\left(\frac{\epsilon}{m_e c^2}\right)^2 = \sigma_{ne^+}\,, \tag{17a}$$

$$\sigma_{n\nu_e} = 1.33\sigma_0\left(\frac{e}{m_e c^2}\right)^2\,, \tag{17b}$$

$$\sigma_{p\bar{\nu}_e} = 1.33\sigma_0\left(\frac{\tilde{e}}{m_e c^2}\right)^2\,, \tag{17c}$$

where $\sigma_0 = 1.7 \times 10^{-44}$ cm^2. The neutrino energy is ϵ, and $e = \epsilon + Q$, $\tilde{e} = e - Q$, with $Q = 0.781$ MeV (the mass difference between a neutron and the sum of the proton and electron masses). Equation (16) simplifies to

$$\left.\frac{\partial F}{\partial t}\right|_{\rm ea} = \frac{2\sigma_{\rm ep}c}{6}\left\{\left(\frac{e}{\epsilon}\right)^2[n_p f_{e^+} N_n(1-f_e)] + \left(\frac{\tilde{e}}{\epsilon}\right)^2[n_n f_{e^+} + n_p(1-f_{e^+})]\right\}(A-F)\,, \tag{18}$$

where

$$\frac{A}{6\alpha\epsilon^3} = \frac{e^2 Z f_e + \tilde{e}^2(1-Z)f_{e^+}}{e^2[Zf_{e^+}(1-Z)(1-f_e)] + \tilde{e}^2[(1-Z)f_{e^+} + Z(1-f_{e^+})]}\,, \tag{19}$$

and Z is the ratio of the number of free protons to the number of free baryons. Note that in the limit where $\mu_\nu = 0$, and where the neutrinos are in equilibrium with the matter, $A/6\alpha\epsilon^3$ will reduce to a thermal Fermi-Dirac distribution function at temperature T. Note that use must be made of the relationship $\mu_n - \mu_p = Q + T \ln(1 - Z/Z)$, where μ_n and μ_p are the chemical potentials of neutrons and protons, respectively.

The final term on the right-hand side of equation (8), $\partial F/\partial t|_{\rm hydro}$, represents the effect of material compression of the neutrino fields as the material moves through space. The exact form of this term is (see Lindquist 1966; Mihalas 1978, p. 501, eqs. [14]–[30])

$$\left.\frac{\partial F}{\partial t}\right|_{\rm hydro} = \frac{F}{\rho}\frac{\partial\rho}{\partial t} + \epsilon\frac{\partial F}{\partial\epsilon}\frac{v}{r} + r\left[\frac{\partial}{\partial r}\left(\frac{v}{r}\right)\right]\epsilon\frac{\partial P_\nu}{\partial\epsilon}\,, \tag{20}$$

where P_ν is the neutrino pressure. We have chosen to approximate equation (20) as

$$\left.\frac{\partial F}{\partial t}\right|_{\rm hydro} = \frac{F}{\rho}\frac{\partial\rho}{\partial t} + \frac{1}{\rho}\frac{\partial\rho}{\partial t}\epsilon\frac{\partial}{\partial\epsilon}\left(\frac{D}{\lambda c}F\right)\,; \tag{21}$$

this reduces to equation (20) in the limit $D/\lambda c = \frac{1}{3}$. In the limit of free streaming neutrinos $D/\lambda c \to 0$, and equation (21) does not reduce to (20); however, if use is made of the fact $v \sim 1/r$ (quasi–free fall) in this region, then equation (21) reduces to equation (20).

IV. RESULTS FOR STELLAR CORE COLLAPSE WITH MAJORONS

In what follows we will briefly outline the salient features of the standard model of stellar collapse and then describe changes in these features due to the effects of using the majoron model of the weak interaction. As outlined above, we will consider three separate implementations of "majoron-like" models of the weak interaction. Model 3 differs from the standard model in that all neutrinos are homogenized and thermalized. Lepton number is not conserved in these interactions, but we assume that no majorons are produced and total neutrino number is conserved. Model 2 is the GRN majoron model, but with the assumption that majoron plus neutrino number changing reactions are negligible on time scales of interest in the collapse. Model 1 uses the GRN majoron model with the assumption that neutrino plus majoron number is not conserved.

The standard model of stellar collapse is principally characterized by the low entropy of the material in the stellar core (Bethe *et al.* 1979). The Fe core of the presupernova star is supported chiefly by the pressure of degenerate electrons and has a mass that is close to the Chandrasekhar mass. The core is destabilized by a combination of electron capture and photodisintegration of iron-peak nuclei. The collapse begins when the central density is of the order of $\rho Y_e \approx 10^{10}$ g cm^{-3}. At this density the stellar core is still transparent to neutrinos but when the central density rises to the order of $\rho Y_e \geq 5 \times 10^{11}$ g cm^{-3} the neutrinos become trapped and begin to thermalize.

It is at this point of neutrino trapping and thermalization that we begin to follow the collapse for the standard model and models 1, 2, and 3 described previously.

In the standard model (all calculations were made using a 1.33 $M_\odot$ Fe core initial model; Weaver, Woosley, and Fuller 1985) the entropy remains low throughout the collapse. If the entropy per baryon in units of Boltzmann's constant is denoted by S, then $S \approx 1$ until the core bounces. Figures 3*a* and 3*b* give values of relevant parameters during the infall epoch in the standard model of collapse. Since the nuclear partition functions are large, and the initial Fe core starts out at low entropy, the nucleons tend to reside in heavy nuclei. Note that the mass fraction in heavy nuclei, X_A, remains on the order of 9% or more throughout the infall epoch. With all but $\leq 10\%$ of nucleons bound in heavy nuclei the Maxwell-Boltzmann pressure of nonrelativistic nucleons and nuclei is small compared to the total pressure. The total pressure is small compared to the pressure required for hydrostatic equilibrium. The

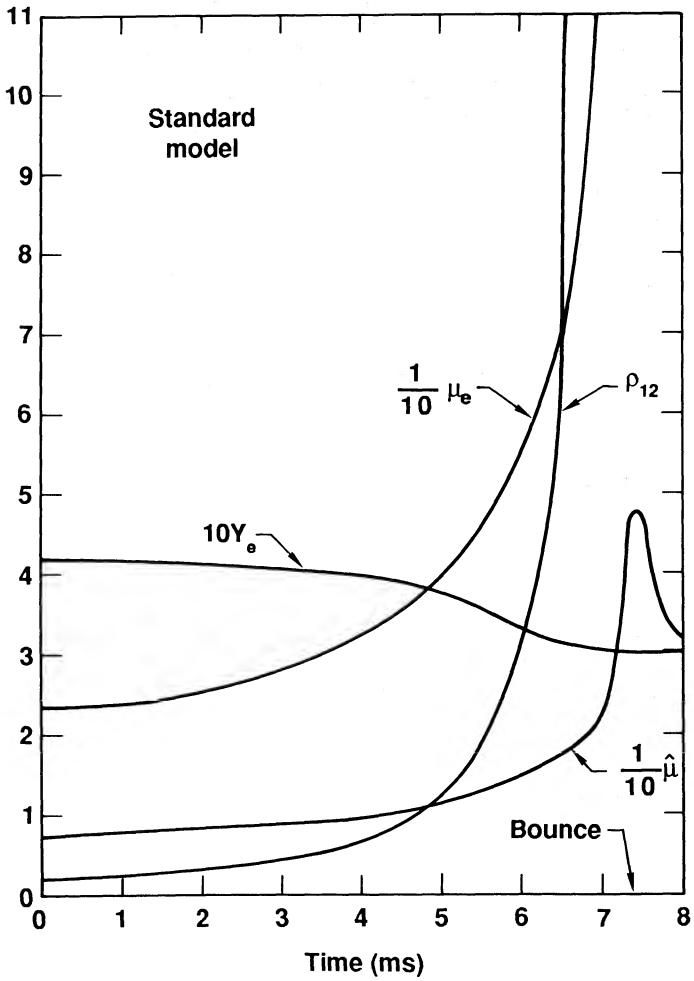

FIG. 3a

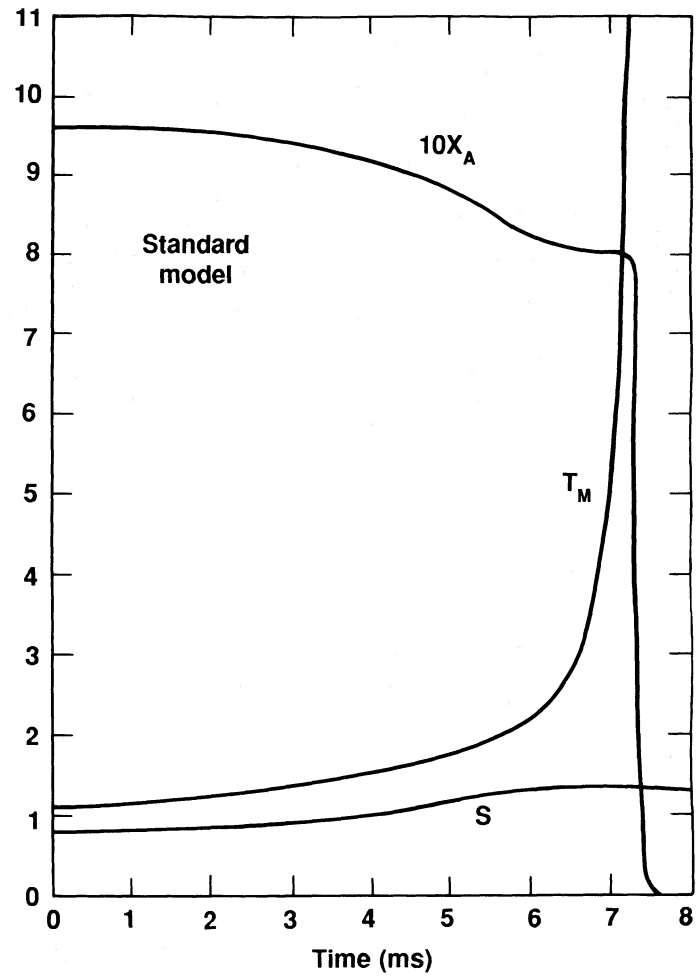

FIG. 3b

FIG. 3.—Composition and lepton physics parameters as a function of time since collapse for the standard model of the weak interaction. Vertical scale is in MeV where appropriate. (*a*) Electron fraction, Y_e, electron chemical potential μ_e (in MeV), neutron-proton chemical potential difference, $\hat{\mu}$ (in MeV), and density ρ_{12} (in units of 10^{12} g cm^{-3}). (*b*) The temperature T_m (in MeV), the entropy-per-baryon S (in units of Boltzmann's constant k), and the mass fraction in heavy nuclei X_A.

net result is that the core collapses at an appreciable fraction of the free-fall rate until the central density of the core is near nuclear density ($\rho_{\rm nuc} \geq 2 \times 10^{14}$ g cm^{-3}). At this point the nuclei merge, and the pressure becomes large as it begins to be dominated by nucleon degeneracy and the nucleon-nucleon force. Only then is the collapse halted with a "bounce" of the core above nuclear density.

The largest contribution to the total pressure during infall comes from the relativistically degenerate electrons. The electron fraction Y_e decreases during the collapse due to electron capture reactions,

$$e^- + p \rightleftarrows n + \nu_e \,, \tag{22}$$

and, as Figure 3*a* shows, it decreases from a value of $Y_e = 0.43$ to $Y_e = 0.3$ near bounce. The electron fraction does not decrease below this value because the electron neutrinos produced are thermalized and give rise to a degenerate sea of ν_e which Pauli blocks reaction (22) and gives rise to an appreciable reverse rate.

In fact, the material remains close to beta equilibrium throughout the infall epoch once the neutrinos are trapped and thermalized. The behavior of the electron chemical potential, μ_e, is shown in Figure 3*a* for the standard model. An approximate expression for the electron chemical potential, or Fermi energy, is

$$\mu_e \approx (11.1 \text{ MeV})(\rho_{10}\, Y_e)^{1/3} \,, \tag{23a}$$

where ρ_{10} is the density in units of 10^{10} g cm^{-3}. A similar expression approximates the electron neutrino chemical potential μ_{ν_e},

$$\mu_{\nu_e} \approx (11.1 \text{ MeV})(2\rho_{10}\, Y_{\nu_e})^{1/3} \,, \tag{23b}$$

where Y_{ν_e} is the number of electron neutrinos per baryon.

If the kinetic chemical potential for neutrinos is denoted by μ_n and the chemical potential for protons is μ_p then the difference is defined to be

$$\hat{\mu} \equiv \mu_n - \mu_p \,. \tag{24}$$

Since strong and electromagnetic equilibrium among nucleons and nuclei is achieved on a time scale short compared to any other time scale in collapse, chemical equilibrium obtains among the nucleons, and, therefore, nucleon chemical potentials are the same inside and outside nuclei. In this case, $\hat{\mu}$ can be interpreted as the difference in neutron and proton Fermi levels in a typical nucleus during collapse. The behavior of $\hat{\mu}$ in the standard model of collapse is shown in Figure 3*a*. Note that as the collapse proceeds the mean nucleus becomes increasingly neutron rich, and, hence, $\hat{\mu}$ increases.

The statement that the material remains close to beta equilibrium (or weak equilibrium) is equivalent to the following relation among the lepton and nucleon chemical potentials,

$$\mu_e - \mu_{\nu_e} \approx \hat{\mu} + \delta m \,, \tag{25}$$

where $\delta m = 1.293$ MeV is the difference in neutron and proton masses.

Although the entropy remains low during the infall epoch in the standard model, there is a considerable amount of thermal energy stored in the excited states of nuclei. The temperature remains low during the collapse ($T \approx 1$ MeV) until the nuclei merge near nuclear density. The merging of the nuclei "releases" the energy stored in the nuclear excited states, and the temperature increases to $T > 10$ MeV. The conversion of infall kinetic energy to random thermal energy in the inner core also increases the temperature.

The energetics associated with stellar core collapse in the standard model runs as follows. The binding energy release of the core in dropping from an Fe–white dwarf configuration to a hot protoneutron star is $\sim 10^{52}$ ergs. Roughly 90% of this energy is converted into the degenerate zero-point energy of the ν_e Fermi sea. Another 10% or so of the binding energy is in the infall kinetic energy of the core and the nuclear excited states. The inner core (or instantaneous Chandrasekhar mass core) bounces as a unit near nuclear density, and a shock is formed near the edge of this core with an initial energy comparable to the infall kinetic energy ($\sim 10^{51}$ ergs).

As the shock moves out through the remainder of the material in the original initial Fe core the shock energy is decreased by photodisintegration of the heavy nuclei in the low entropy material streaming through the shock. Whether or not this prompt shock has enough energy to continue moving down the stellar density gradient or whether it stalls and becomes an accretion shock is a matter of current research interest (see Cooperstein 1988; Baron *et al.* 1988).

In any case, after bounce and shock passage the material has its entropy raised to $S \sim 10$, and the nuclei are melted to free nucleons and alpha particles. With the increase in temperature, neutrino pairs (ν_e, $\bar{\nu}_e$; ν_μ, $\bar{\nu}_\mu$; ν_τ, $\bar{\nu}_\tau$) are formed in equilibrium. At this point the core begins to deleptonize from a neutrino "photosphere" located where the density falls to $\rho \sim 10^{11}$ g cm^{-3} (technically there are different photospheres for each of ν_e, $\bar{\nu}_e$, ν_τ, and ν_μ, and we refer the reader to Mayle and Wilson 1987 for further discussion).

The early time ν_e luminosity from this photosphere is shown in Figure 4. The thermal neutrinos come out on a longer time scale. The average energy for ν_e, $\bar{\nu}_e$, and ν_μ are shown as a function of time after bounce in Figure 5. We show only the first few tens of milliseconds because, as will be shown, the nonstandard weak interaction models give very different behavior on this time scale. The thermal neutrino luminosities and energies remain high for several seconds (see Mayle and Wilson 1987) as the hot protoneutron star deleptonizes. In general, the predictions from the standard model for neutrino luminosities and energies are in excellent agreement with the Kamiokande and IMB results for SN 1987A (Mayle and Wilson 1987).

In model 3 we assume that the neutrino-neutrino cross section is larger than in the standard weak interaction with a value comparable to what is expected with the majoron model (eq. [6]) and with the associated lepton number violation. However, we assume that no majorons are produced. Figures 6*a* and 6*b* give the time history of the relevant parameters of stellar collapse as discussed above for the standard model.

The primary effect of the increased neutrino-neutrino scattering cross section and lepton number violation is that as soon as the neutrinos begin to be trapped they are rapidly thermalized at a temperature T_ν on a time scale short compared to a weak interaction time. Of course, the neutrinos principally interact only with other neutrinos so that T_ν is different from, and in fact greater than, the matter temperature T_M.

Neutrinos interact with other neutrinos through the relatively strong "majoron" exchange, whereas neutrinos "feel" the matter only through the standard strength weak interaction. As a result, the nutrino temperature T_ν relaxes to the matter temperature T_M only on the long weak equilibrium time scale.

Since the neutrinos are trapped earlier, and thus the collapse becomes adiabatic sooner, there is a larger share of the gravitational binding energy contained in the neutrino Fermi sea than in the standard model. As the processes of electron capture, neutrino capture, and neutrino-electron scattering drive the system toward weak equilibrium (and $T_\nu = T_M$) entropy is generated (for a discussion of entropy generation in electron capture processes, see Fuller 1982).

The extra entropy generation over the standard model is about $\Delta S \approx 1$ which is enough to only partially melt the nuclei. The nuclear mass fraction, X_A, thus drops somewhat compared to the standard model, bottoming out near $X_A = 60\%$. Since the nuclei partially melt there are more free protons to capture electrons, and, hence, the electron fraction falls to $Y_e = 0.2$.

Nevertheless, in model 3 there is not enough melting of nuclei to increase the pressure compared to the standard model substantially, nor is there enough electron capture to alter the lepton physics significantly. In fact, these effects tend to compensate each other by giving a pressure increase in the former process which is comparable to the pressure decrease in the latter process.

The net result is that the core of model 3 again falls to nuclear density before the collapse is halted, and a shock wave is generated. The energy in this shock is slightly less than in the standard model. The subsequent neutrino emission from the neutrino photosphere is comparable to that in the standard model, as shown in Figure 7.

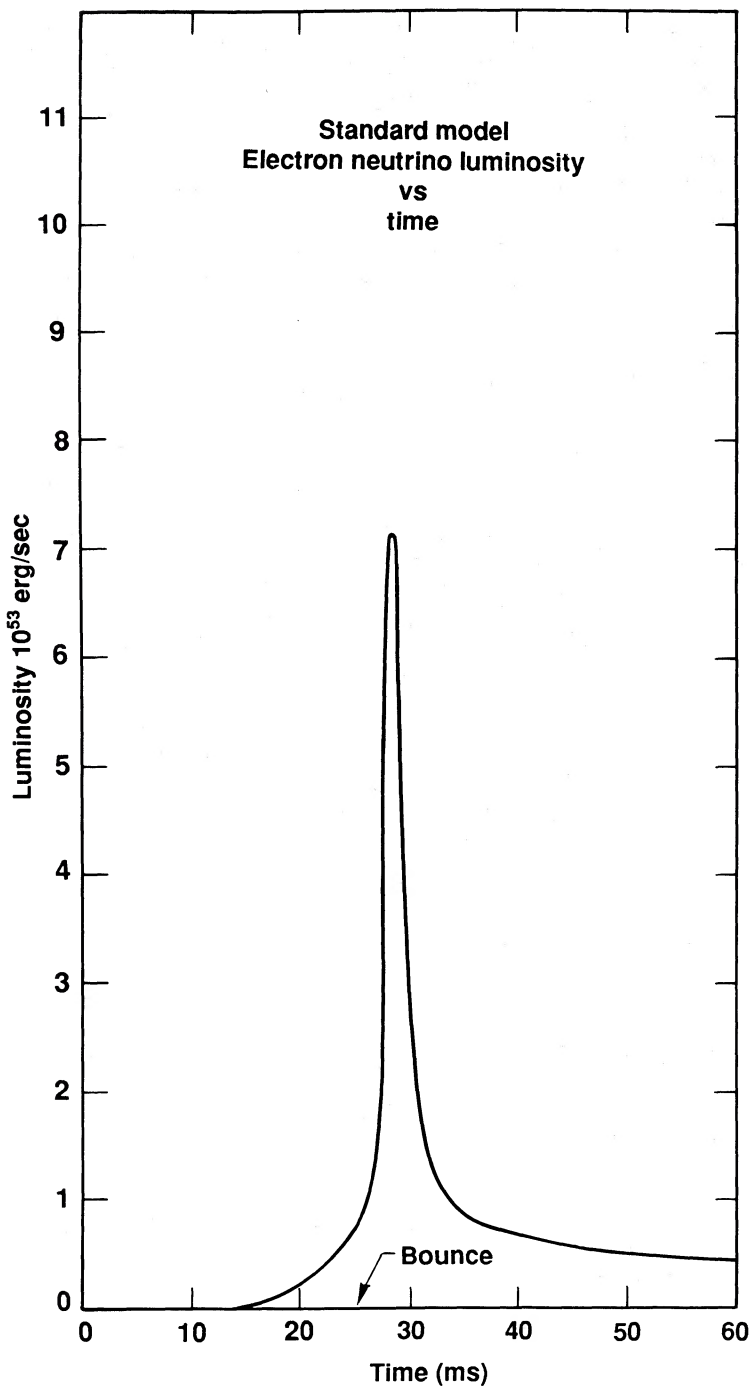

FIG. 4.—Electron neutrino luminosity (in 10^{53} ergs s^{-1}) as a function of time since collapse for the standard model of the weak interaction. The time of core bounce is indicated.

The collapse of model 2 appears to be very different in detail from the standard model. In model 2 the neutrinos interact with each other through the GRN majoron model. Here, again, lepton number is not conserved. We have assumed that $10^{-5} \leq g \leq 10^{-4}$ so that neutrino-neutrino interactions are dominated by majoron exchange, yet the number changing processes are slow compared to other time scales in collapse, and, thus, the total neutrino plus majoron number is conserved.

As in model 3, as soon as the neutrinos begin to be trapped, they are rapidly thermalized by majoron exchange. Unlike model 3 the two-to-two processes shown in Figures 1*b* and 1*c* rapidly build up a thermal distribution of majoron particles ϕ and ρ. Again the neutrino temperature T_ν is different than the matter temperature T_M. As before, T_ν relaxes to T_M only on a long weak equilibrium time scale.

Lepton number violation ensures that the ν_e produced by electron capture are converted to $\bar{\nu}_e$, ν_μ, $\bar{\nu}_\mu$, ν_τ, $\bar{\nu}_\tau$ and ϕ on a majoron interaction time scale. The neutrino chemical potentials are now equal, but, as discussed in § III, μ_ν is small and negative, as is μ_ϕ.

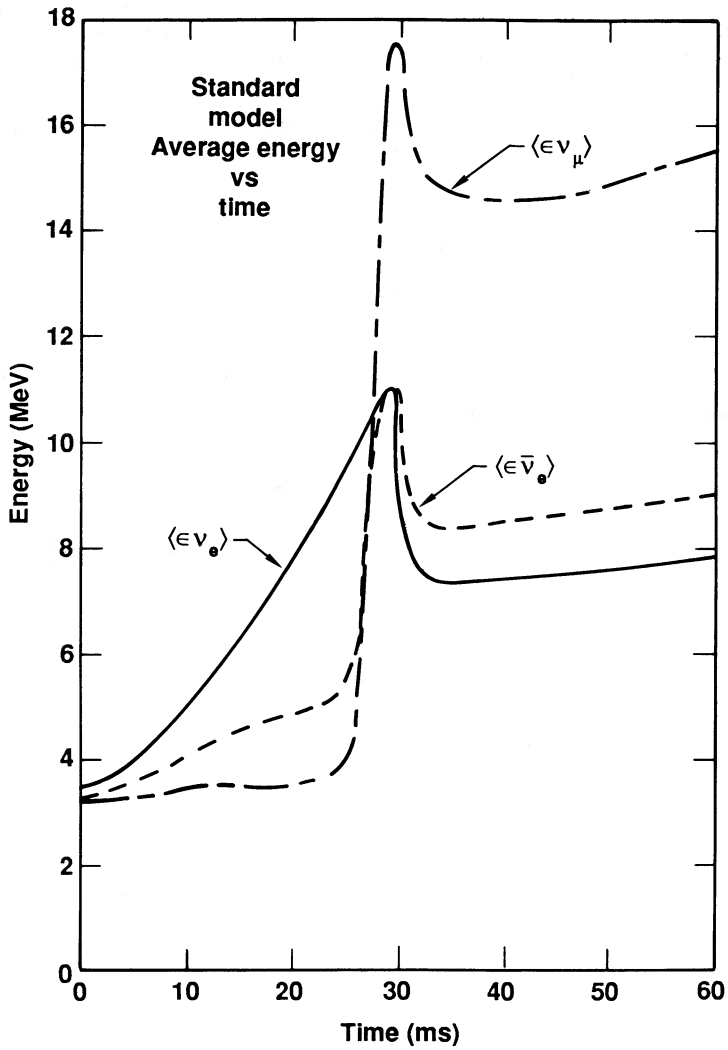

FIG. 5.—Average electron neutrino energy $\epsilon\nu_e$, muon neutrino energy $\epsilon\nu_\mu$, and, anti–electron-neutrino energy $\epsilon\bar{\nu}_e$ as a function of time since collapse for the standard model of the weak interaction.

Since now the neutrinos are in equilibrium with a majoron gas, the neutrino numbers are reduced, and there is little blocking of reaction (22) by degenerate neutrinos.

Since μ_{ν_e} is now near zero the system is badly out of beta equilibrium, as equation (25) is unbalanced by the rapid majoron interactions. The relevant collapse parameters are shown, as above, for model 2 in Figures 8*a* and 8*b*. With electron capture now unblocked, the electron fraction Y_e falls drastically to $Y_e = 0.05$, where a new beta equilibrium is established. The electron capture reactions, and scattering processes, which drive the system back toward beta equilibrium result in a large entropy generation: $\Delta S \approx 3$.

This increase in entropy is enough to melt the heavy nuclei completely. The matter temperature, T_M, remains roughly constant at ~ 1 MeV until the nuclei melt, whereupon it rises to 8 MeV. The increase in the number of nonrelativistic nucleons and nuclei (all contributing a $\Gamma \approx 5/3$ Maxwell-Boltzmann pressure) plus the associated increase in temperature lead to a large pressure increase which halts the collapse at a density well below nuclear density. The core has a thermal bounce at a density $\rho \approx 2 \times 10^{13}$ g cm^{-3}.

The neutrino luminosity as a function of time after bounce for model 2 is shown in Figure 7. In short, model 2 has a neutrino burst signature which is similar to the standard model at early times and therefore, potentially, consistent with the IMB and Kamiokande neutrino detections for SN 1987A.

It is interesting to speculate on the fate of the core of model 2. The bounce occurs at a central density of $\rho \approx 2 \times 10^{13}$ g cm^{-3}, and a weak shock is formed at the edge of the homologous core. Since the nuclei in the core have already been photodissociated by the entropy generation associated with lepton number nonconservation, we expect little shock energy dissipation subsequent to the bounce. The radius–time history for the central zones of the standard model is shown in Figure 9*b*, while the analogous plot for model 1 is shown in Figure 9*a*. As will be discussed below, the radius–time history for model 2 is very similar to model 1.

Finally, in model 1, we consider the case in which $g \geq 10^{-4}$ for the GRN majoron model. Model 1 has essentially the same lepton physics as model 2 but with the added feature that the number changing processes in Figures 2*a*–2*c* are now assumed to be fast compared to a weak equilibrium time scale. In model 1 not only is lepton number not conserved, but the total neutrino plus

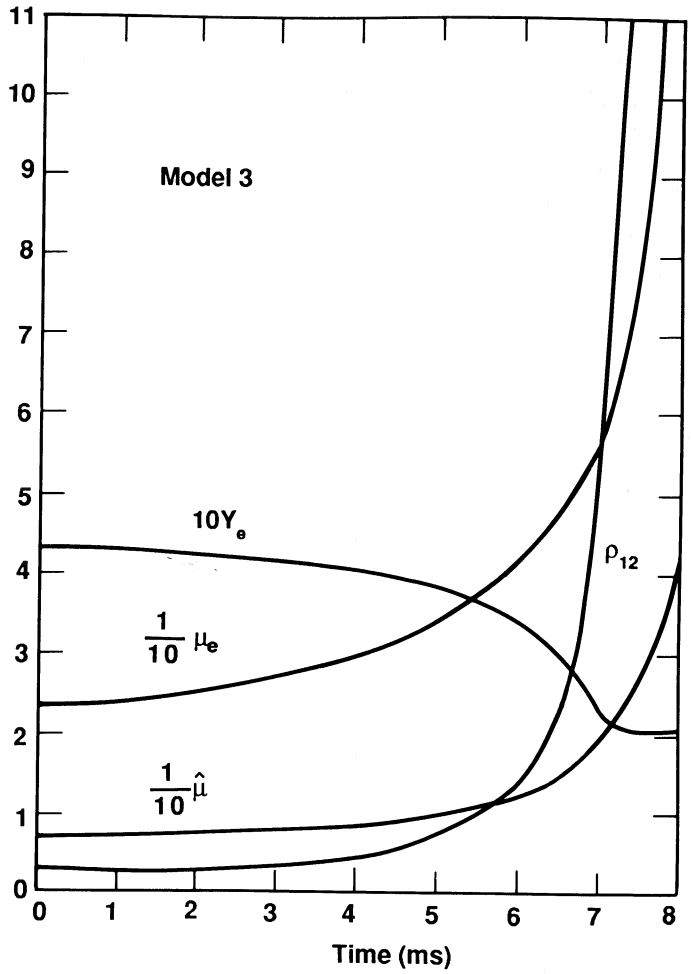

FIG. 6a

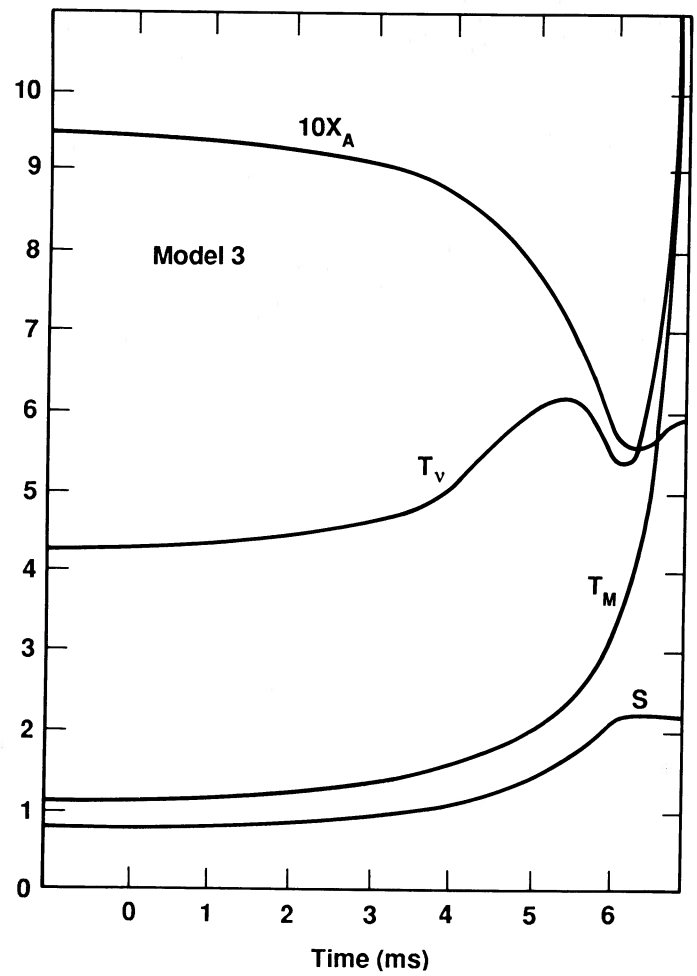

FIG. 6b

FIG. 6.—Collapse physics parameters as a function of time as in Figs. 3a, 3b, but now for model 3: (a) Y_e, μ_e, $\hat{\mu}$, and ρ_{12}; (b) X_A, S, T_ν, and T_M

majoron number is not conserved either. The composition, density, temperature for majorons and neutrons (T_ν) and the matter temperature (T_M) along with the relevant lepton physics parameters (Y_e, μ_e, $\hat{\mu}$) are shown for the collapse and bounce of model 1 in Figures 10a and 10b. In broad character the behavior of these parameters is quite similar to that in model 2: entropy generation associated with lepton number nonconservation ($\Delta S \approx 3$); melting of the nuclei and large amounts of electron capture (finally $Y_e \approx 0.04$), followed by a thermal bounce at subnuclear density ($\rho_{\text{bounce}} \approx 2 \times 10^{13}$ g cm^{-3}). The entropy generation in model 1 is only slightly greater than in model 2.

Model 1, unlike model 2, allows the total neutrino plus majoron number to change. Since neutrinos and majorons are produced in profusion, all neutrino and majoron chemical potentials are equal, and, with no number conservation, rigorously $\mu_\nu = \mu_\phi = 0$. This is the condition originally discussed by Kolb, Tubbs, and Dicus (1982). More neutrinos and majorons in thermal equilibrium implies that the gravitational binding energy of the core is shared over more thermal degrees of freedom. Thus, we expect the average neutrino and majoron energies in the core to be lower.

We will now discuss the nature of the neutrino flux exterior to the photosphere for model 1. Inside the photosphere we assumed majoron mediated reactions were swift enough to put the neutrinos in a Fermi-Dirac distribution. This will be true for any coupling, g, great enough to be of interest (a few $\times 10^{-5}$). In Figure 7 the luminosity at the photosphere versus time is shown for the three models. It is seen that after the core settles down subsequent to bounce, the luminosities level out at $\sim 10^{53}$ ergs s^{-1}. Presumably the luminosities will slowly decrease over a period of several seconds as the protoneutron star cools. In Figure 11 the mean energy of the neutrinos at the photosphere is given for the three calculations. It is to be expected that the mean energies of models 2 and 3 will increase with time as the core contracts and rises in temperature. The average energy of the neutrinos averaged over the full time of emission is expected to be greater than 15 MeV. This is somewhat hotter than the average of the three species energies shown in Figure 5. Outside the photosphere (defined as the radius of last mean interaction of neutrinos with electrons and baryons) the neutrinos are still interacting with each other. The majoron neutrino cross section varies inversely with the square of the energy, and, if the interaction is strong enough, the neutrinos will expand and cool as a gas. Since total number is not conserved, a large number of neutrinos plus majorons of low energy could be the result at large distances. To study the exterior behavior of the neutrinos, we take a very simple model valid just outside the photosphere. Assume that at the photosphere all neutrinos below a

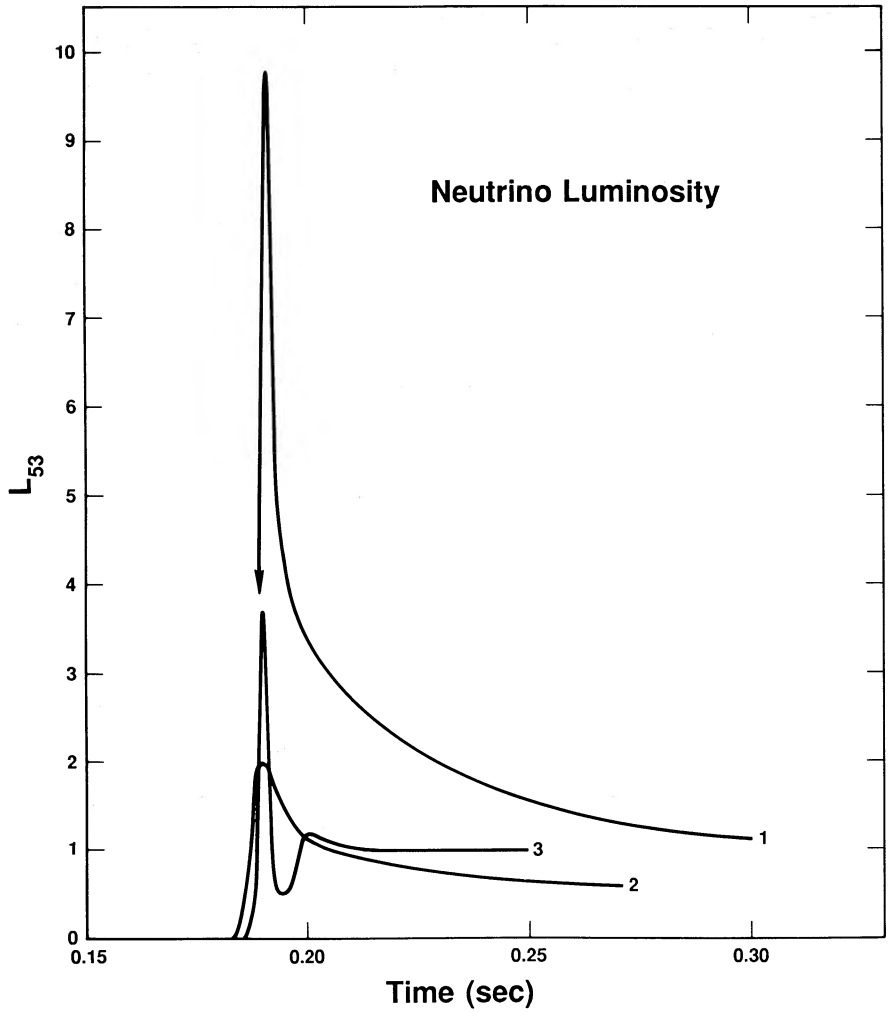

FIG. 7.—Neutrino luminosity (in 10^{53} ergs s^{-1}) as a function of time since collapse for models 1, 2, and 3

critical energy E_c behave like a gas in thermal equilibrium and that all neutrinos above energy E_c escape to infinity unscathed. Further, to make the integrals easy, we suppose the neutrinos and majorons are in a Boltzmann distribution at the photosphere and

$$L \approx 4\pi r_p^2 \frac{acT_p^4}{4} \frac{n}{2}, \tag{26}$$

with $n = 7$. The number density, N_0, and mean energy, $\bar{E}_0$, of low-energy neutrinos at the photosphere is

$$N_0 = \int_0^{E_c} N(\epsilon) d\epsilon = \frac{anT^4}{6T}\left[1 - e^{-x}\left(1 + x + \frac{x^2}{2}\right)\right], \tag{27a}$$

$$\bar{E}_0 = T\{6 - e^{-x}(x^3 + 3x^2 + 6x + 6)/[2 - e^{-x}(x^2 + 2x + 2)]\}, \tag{27b}$$

where $x = E_c/T$ and a is a constant. At any other radius the low-energy neutrinos are characterized by

$$N(r) \approx N_0(r_p/r)^{3/2}, \tag{28a}$$

$$\bar{E}(r) \approx \bar{E}_0(r_p/r)^{1/2}. \tag{28b}$$

To define E_c we let $\sigma = (g^2/4\pi)^2(\hbar c/E)^2$ and fix E_c by

$$\int N(r)\left(\frac{g^2}{4\pi}\right)^2\left(\frac{\hbar c}{4\pi}\right)^2 dr = 1 = 2N_0 r_p\left(\frac{g^2}{4\pi}\right)^2\left(\frac{\hbar c}{E_c}\right)^2. \tag{29}$$

For a Boltzmann distribution the fraction of the total neutrino energy composed of neutrinos of energy greater than E_c is

$$f = e^{-x}\left(1 + x + \frac{x^2}{2} + \frac{x^3}{3}\right). \tag{30}$$

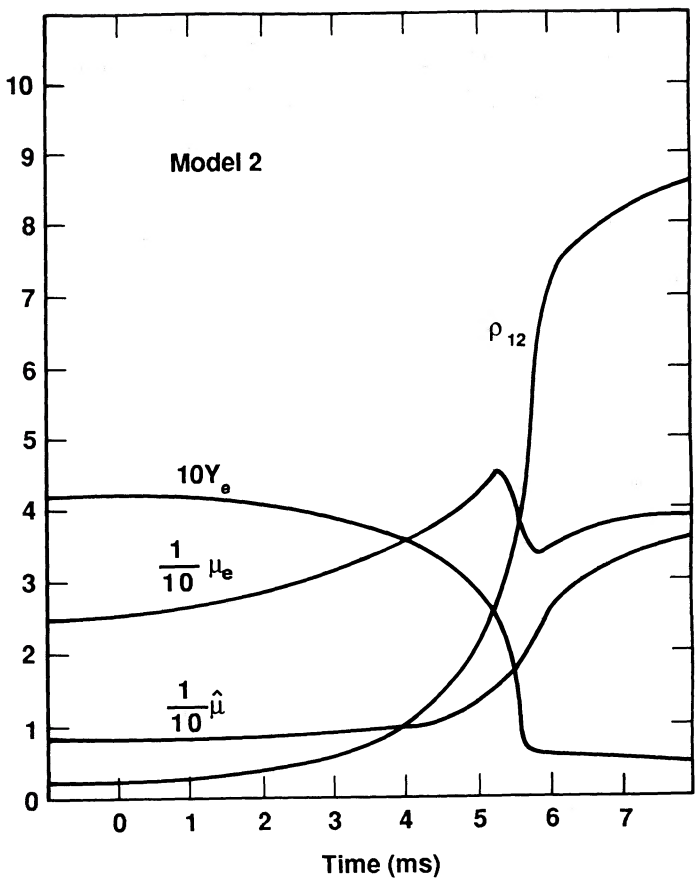

FIG. 8*a*

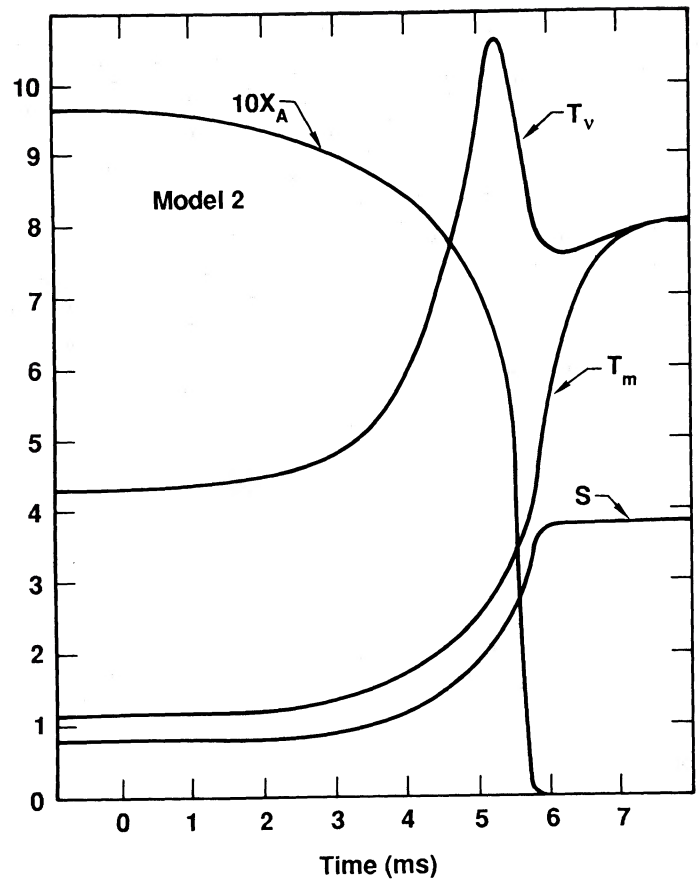

FIG. 8*b*

FIG. 8.—Collapse physics parameters as a function of time as in Figs. 6*a*, 6*b*, but for model 2: (*a*) Y_e, μ_e, $\hat{\mu}$, and ρ_{12}; (*b*) X_A, S, T_v, and T_M

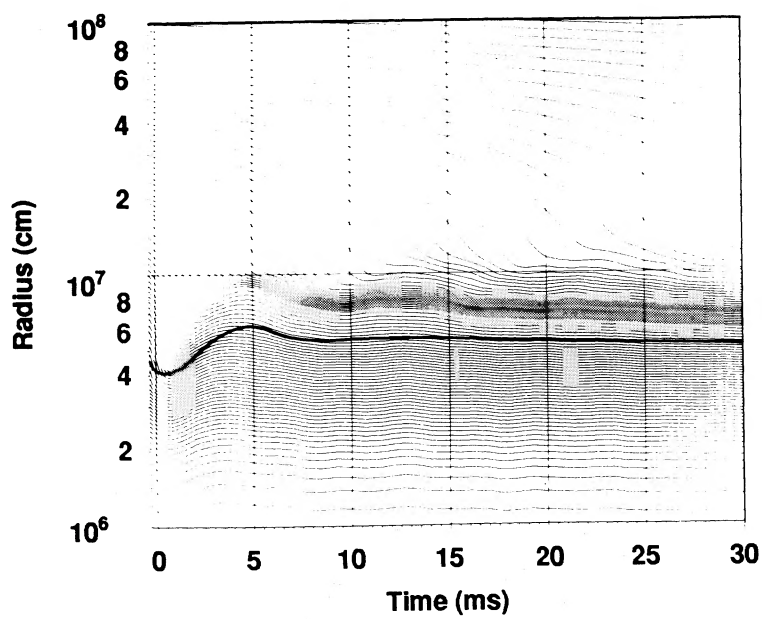

FIG. 9*a*

FIG. 9.—Radius (in cm) for the inner zones of the star is shown as a function of time since collapse for (*a*) model 1 and (*b*) the standard weak interaction model. Heavy line indicates the edge of the core.

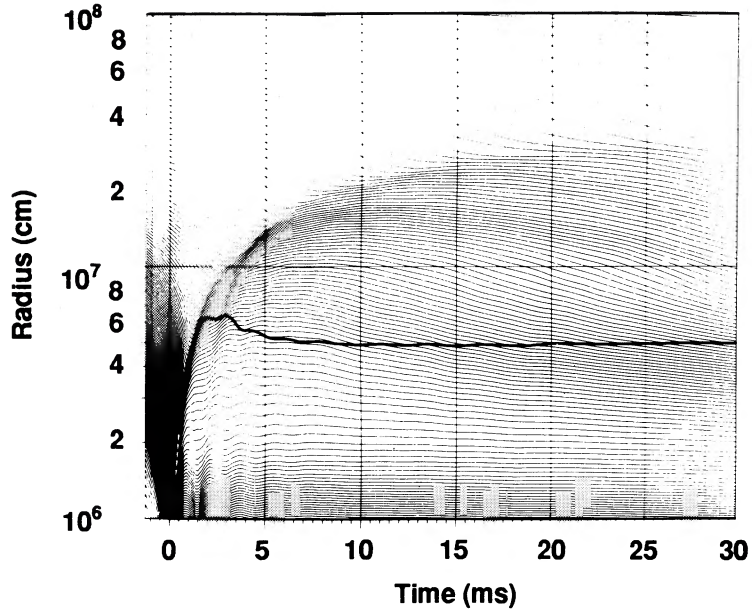

FIG. 9*b*

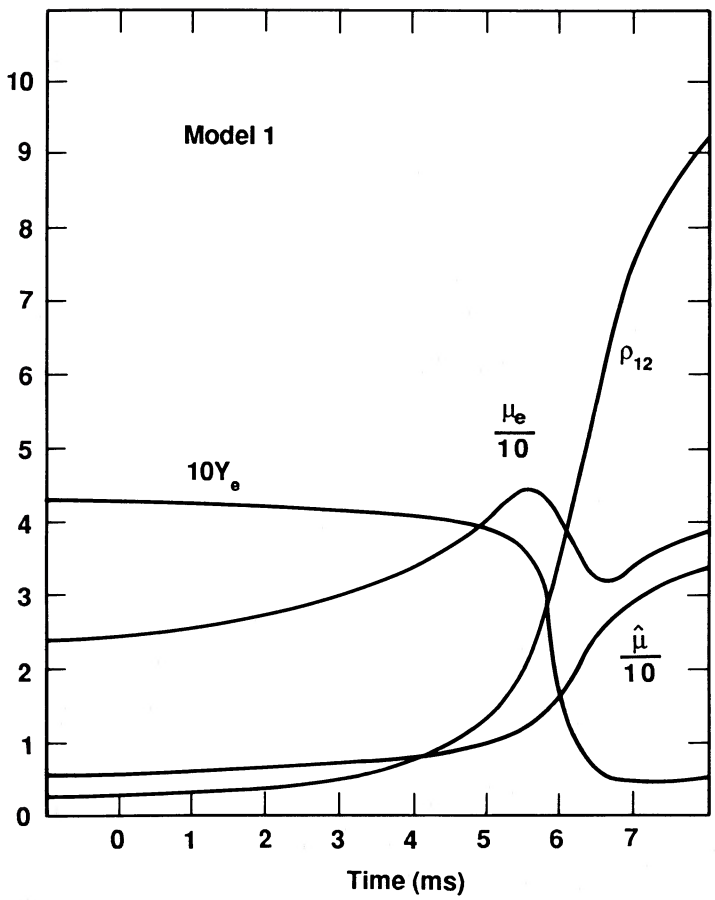

FIG. 10*a*

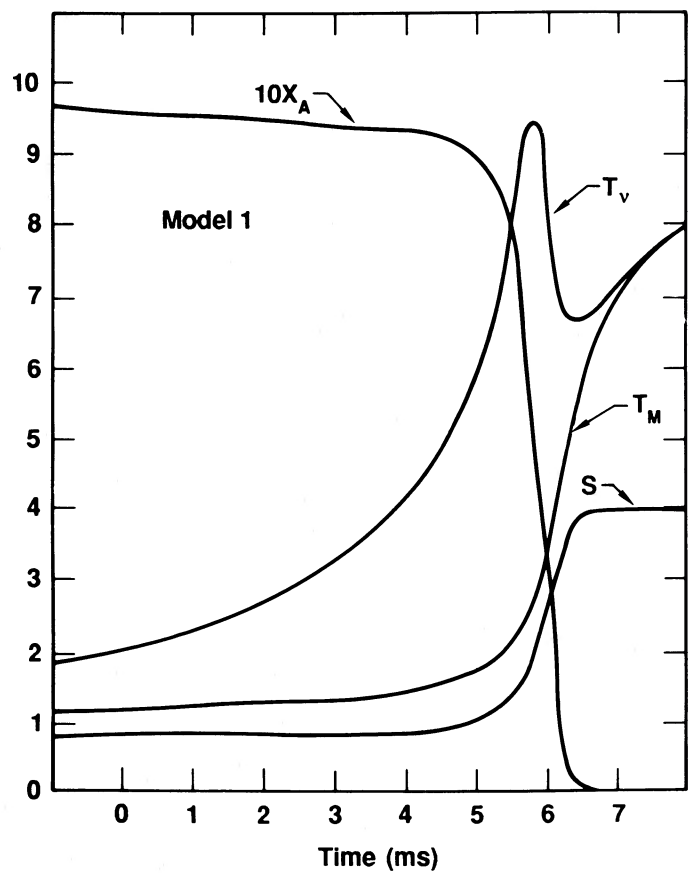

FIG. 10*b*

FIG. 10.—Collapse physics parameters as a function of time as in Figs. 3*a*, 3*b*, but now for model 1: (*a*) Y_e, μ_e, $\hat{\mu}$, ρ_{12}; (*b*) X_A, S, and now the matter temperature T_M (in MeV) and the neutrino and majoron temperature T_ν (in MeV).

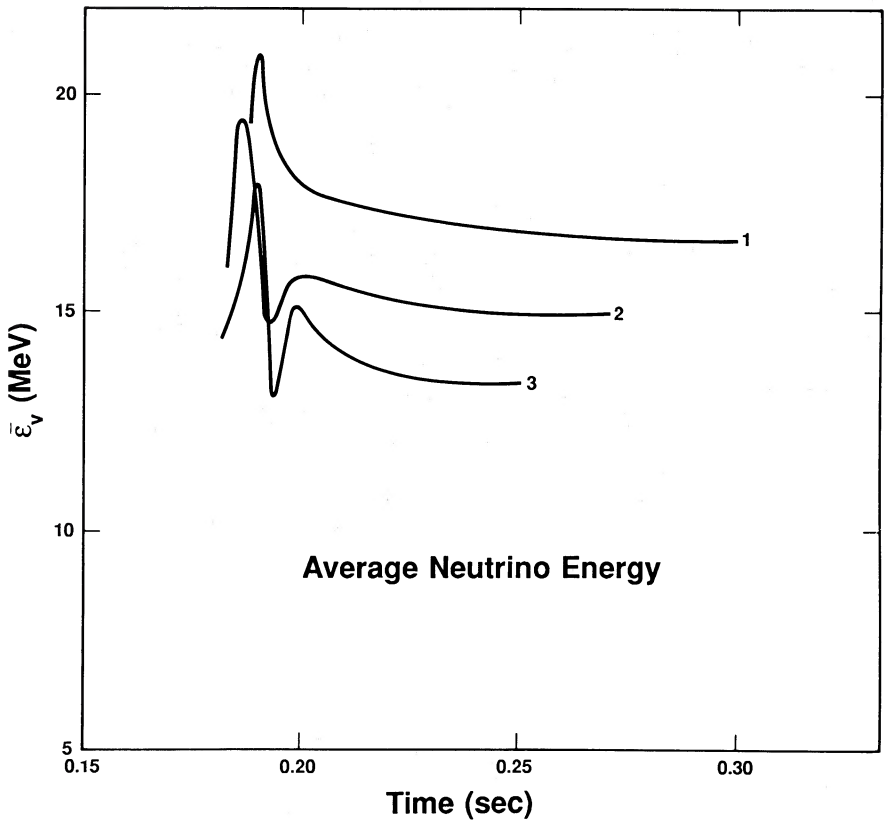

FIG. 11.—Average neutrino energies vs. time for models 1, 2, and 3

Now with luminosity equal 10^{53} ergs s^{-1} and T equal 5 MeV, we plot coupling constant g versus fraction of escaping energy f in Figure 12. The curve is very steep; hence, it is clear that SN 1987A restricts g to be less than $\sim 3 \times 10^{-4}$. A 50% increase in the number of neutrinos would reduce the antineutrino energy such as to be incompatible with SN 1987A observations. For a comparison of the stardard model with IMB and Kamiokande see Mayle and Wilson (1987). This value of g is also close to the minimum value of g from the double decay experiments (Avignone *et al.* 1987; Caldwell 1988; Elliot, Hahn, and Moe 1987; Alston-Garnjost *et al.* 1987). Aharonov *et al.* (1988*a*, *b*) have discussed majoron production and decay above and below the photosphere after a standard model collapse and bounce. They found consistency of the subsequent neutrino burst with that of SN 1987A even if g is $\sim 7 \times 10^{-4}$. This is similar to our result, except in the extreme modification inherent in the infall epoch for model 1.

If the coupling is strong enough to equilibrate the neutrinos under the photosphere but small enough to allow the neutrinos to maintain their energy after passing above the photosphere, then the late time heating mechanism has a better chance of working than in the standard model. This is because the average energy of the electron neutrinos and antineutrinos (which are the principal contributors to late time heating) is higher in the majoron model than in the standard model. If the coupling constant were much greater than the critical value (3×10^{-4}), it might be possible to have a neutrino signal that could give rise to the Mount Blanc type signal, i.e., large number of neutrinos at reduced energy. However, we cannot account for both Mount Blanc and Kamiokande, or IMB in a single model.

V. CONCLUSION

We have studied the collapse and bounce of the Fe core of a presupernova star with the standard model of the weak interactions and with the Gelmini-Roncadelli-Glashow-Georgi-Nussinov majoron model of the weak interaction. We have confirmed in broad outline the speculations of Kolb, Tubbs, and Dicus (1982) as to the effect of the majoron picture on the standard low-entropy model of stellar collapse: entropy generation associated with lepton number nonconservation, melting of the heavy nuclei, and a thermal bounce of the core at subnuclear density. The details of these processes can be quite different than as described in previous work.

The thermal bounce of the core could be followed by an explosion generated by a late-time neutrino heating mechanism. We indentify the rate of neutrino and/or majoron number changing reactions as the principal determinant of the neutrino characteristics associated with such explosions. In particular, for $g \geq 3 \times 10^{-4}$ the total neutrino plus majoron number is not conserved, and also the neutrino energies are too low to be consistent with the neutrino observations from SN 1987A. In the relatively narrow parameter range $10^{-5} \leq g \leq 3 \times 10^{-4}$ the majoron model could conceivably give a thermal bounce supernova with a neutrino signal marginally consistent with SN 1987A. However, we emphasize that this is indeed a narrow parameter range, and a more detailed treatment of the neutrino plus majoron number changing process than presented here may yield a different result.

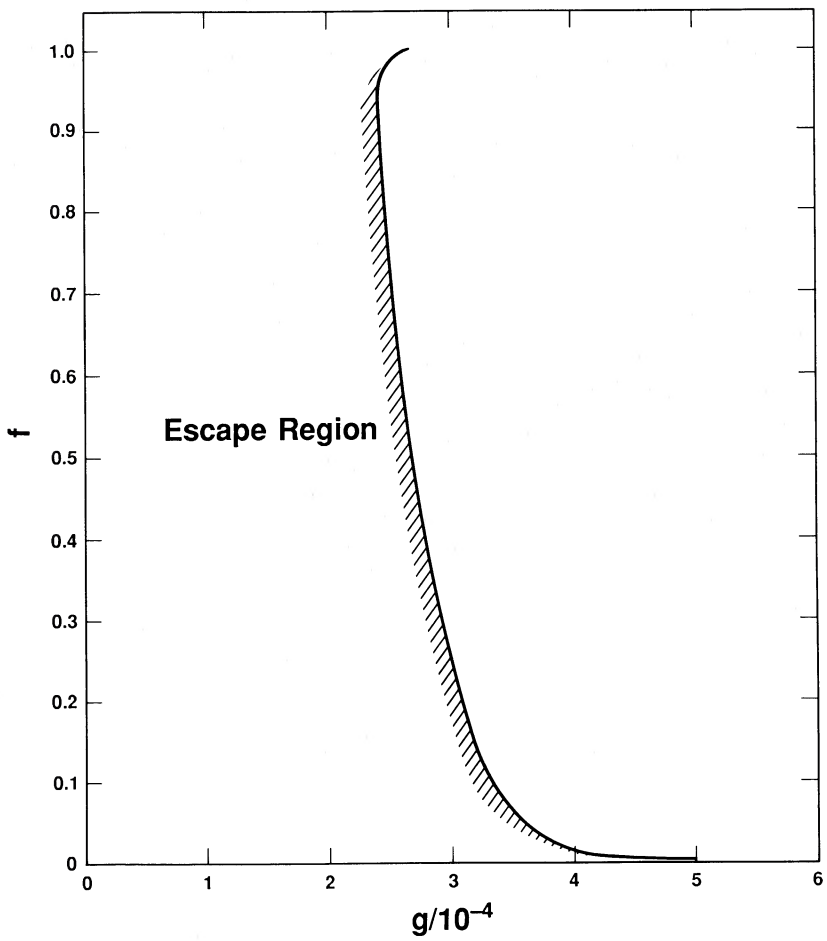

FIG. 12.—Fraction of neutrinos escaping to infinity with undegraded energy vs. coupling strength, g

Finally, even if the lepton number symmetry is restored when the core is heated to $T \approx 10$ MeV we find the majoron model would have already produced the indicated effects of entropy generation and large amounts of electron capture. "Turning off" the lepton number nonconservation at this point would have little effect on our results.

The authors acknowledge useful discussions with C. R. Alcock, F. Avignone, J. Frieman, and D. Seckel. Work performed under the auspices of the US Department of Energy by Lawrence Livermore National Laboratory under contract No. W-7405-ENG-48.

REFERENCES

Aharanov, Y., Avignone, F. T., and Nussinov, S. 1988*a*, *Phys. Letters*, in press.
———. 1988*b*, *Phys. Rev. D*, in press.
Alston-Garnjost, M., Dougherty, B., Kenney, R., Krivicich, J., Trip, R. 1988, *Phys. Rev. Letters*, submitted.
Avignone, F. T., Brodzinski, R. L., Miley, H. S., and Reeves, J. H. 1987, preprint.
Baron, E., Cooperstein, J., and Khana, S. 1988, preprint.
Bethe, H. A., Brown, G. E., Applegate, J., and Lattimer, J. M. 1979, *Nucl. Phys. A*, **324**, 487.
Bionta, R. M., *et al.* 1987, *Phys. Rev. Letters*, **58**, 1494.
Bowers, R. L., and Wilson, J. R. 1982, *Ap. J. Suppl.*, **50**, 115.
Caldwell, D. 1988, private communication.
Cooperstein, J. 1988, preprint.
Dicus, D. A., Kolb, E. W., and Tubbs, D. L. 1983, *Nucl. Phys. B*, **223**, 532.
Elliot, S. R., Hahn, A. A., and Moe, M. K. 1987, *Phys. Rev. Letters*, **59**, 1649.
Frieman, J. 1987, SLAC preprint.
Fuller, G. M. 1982, *Ap. J.*, **252**, 741.
Fuller, G. M., Mayle, R., Wilson, J. R., and Schramm, D. N. 1987, *Ap. J.*, **322**, 795.
Gelmini, G. B., and Roncadelli, M. 1981, *Phys. Letters*, **99B**, 411.
Georgi, H. M., Glashow, S. L., and Nussinov, S. 1982, *Nucl. Phys. B*, **193**, 297.
Grinstein, B., Preskill, J., and Wise, M. B. 1985, *Phys. Rev. Letters*, **159B**, 57.
Haxton, W. C., Stephenson, G. J., and Strottman, D. 1981, *Phys. Rev. Letters*, **46**, 698.
Hirata, K., *et al.* 1987, *Phys. Rev. Letters*, **58**, 1490.
Kolb, E. W., Tubbs, D. L., and Dicus, D. A. 1982, *Ap. J.* (*Letters*), **225**, L57.
Lindqist, R. W. 1966, *Ann. Phys.*, **37**, 487.
Mayle, R. 1985, UCRL Rept. 53713.
Mayle, R., and Wilson, J. R. 1987, preprint.
Mihalas, D. 1978, *Stellar Atmospheres* (San Francisco: Freeman).
Tubbs, D. L., and Schramm, D. N. 1975, *Ap. J.*, **201**, 467.
Weaver, T. A., Woosley, S. E., and Fuller, G. M. 1985, in *Numerical Astrophysics*, ed. J. Centrella, J. Leblanc, and R. Bowers (Boston: Jones & Bartlett), p. 374.

G. M. FULLER, R. MAYLE, and J. R. WILSON: Lawrence Livermore National Laboratory, P.O. Box 808, Livermore, CA 94550